AIAA AVIATION Forum
June 25-29, 2018, Atlanta, Georgia
2018 Multidisciplinary Analysis and Optimization Conference

10.2514/6.2018-2924

Increasing Conceptual Design Fidelity with Prebuilt Airfoil Databases

Timothy MacDonald*, Juan J. Alonso†
Stanford University, Stanford, CA 94305, USA

Due to time and monetary constraints, the conceptual design process for new aircraft is typically limited to inexpensive low-fidelity methods. Unfortunately, these methods generally only provide the fidelity necessary to confidently go forward with a new design when they have been fitted to previous aircraft of the same type. The conceptual design process has difficulty producing accurate estimates of performance in unconventional aircraft. To remedy this, new methods must be developed that can produce higher fidelity results without a significant increase in cost. Here we present a method to do this in the aerodynamic analysis. First, we generate a large database of airfoils that are optimized using CFD to minimize drag in a variety of flight conditions that are likely to be seen on the wing of a subsonic transport aircraft. We then present methods to integrate these airfoils along an arbitrary wing to find the minimum possible drag. This process is meant to mimic the "expert designer" often pointed to in current correlation equations for determining the drag of a wing. Since the airfoils are generated before hand in a manner that is easy to parallelize, this process is not substantially more expensive than other methods for determining the aerodynamic properties of an aircraft at the conceptual level.

I. Introduction

The conceptual design process must be sufficiently reliable that an aircraft manufacturer can be sure that gains shown at this stage are realizable in the final design, but must also be fast enough that a large design space can be explored. For the conventional tube and wing configurations, this problem is made substantially easier by many years of accumulated data. This data means that accurate correlations can be created and used in the process. Unfortunately these methods are not effective in the design of less conventional configurations that are necessary to achieve more than marginal increases in performance. In order to build accurate models of unconventional configurations, analysis tools must be able to account for the underlying physics. Furthermore, while sophisticated physical models exist, they are often too computationally expensive.

Here we attempt to address this computational expense in the aerodynamic realm. To do this, we build a database of optimized airfoils that can then be used to estimate drag for a 3D wing. Typical drag values for aircraft wings are based on previous wings under the assumption that this is what an expert designer will be capable of creating. The optimized airfoils will give us a similar sort of baseline, allowing us to take the role of the expert designer and give an expected value for the drag of the final full wing. This paper is organized as follows: Section II describes the general capabilities and software used, Section III shows the methodology of this process, Section IV gives demonstration cases, and finally Section V provides a summary of these results.

II. Capabilities Background

In order to perform this type of analysis and evaluate the results, we must have tools capable of airfoil and wing optimization. Fortunately the basics of these capabilities exist within tools that are readily available.

*Graduate Student, Department of Aeronautics and Astronautics, AIAA Student Member.
†Professor, Department of Aeronautics and Astronautics, AIAA Associate Fellow.

A. Pointwise

Pointwise is a commonly used mesh generation program that can be used for both airfoils and 3D wings. A key feature of this tool is the ability to automatically mesh geometries based on a premade script. A script of this sort is used in meshing airfoils so that airfoils of arbitrary thickness can be generated as needed by the chosen sampling algorithm. In addition, Pointwise can automatically export mesh files into SU2 format, which is a code base described below.

B. SU2

The SU2 software suite[1] is an open-source collection of software tools written in C++ and Python for performing multi-physics simulation and design. As part of this, it has the capability to do shape optimization of both airfoils and full wings (or even aircraft). Airfoil optimization options include Hicks-Henne bumps and free-form deformation (FFD) boxes. We have chosen Hicks-Henne bumps for the work in this paper. The open-source nature of SU2 has also allowed us to implement new airfoil optimization functions as needed.

C. SUAVE

SUAVE[2] is an open-source conceptual design tool built to handle unconventional configurations in a modular way. It is written in Python, making it easy to import various modules as needed. In this case, its aerodynamics analyses and plugins are used to support calculations that SU2 does not provide. It is also eventually intended to serve as the driver for aircraft analysis using the methods in this work.

III. Methods

A. General Method

In order to build a 3D model from 2D slices, we first need a way to find the properties of those 2D slices. Since we want to predict performance consistent with the results of an expert design team developing a wing, we cannot simply pull data from existing airfoils. Instead, we begin by optimizing airfoils for a variety of conditions that may be required by the geometry of the wing and seen in flight. We have chosen the parameters of thickness to chord, Mach number, and necessary section coefficient of lift. This is consistent with previous work we have found on the subject, which we hope to improve upon in part with the layout of a detailed methodology.[3]

Once an optimized family of airfoils is created, a surrogate must be made that can be used to generate airfoil properties (drag in this case) in conditions that have not been explicitly calculated. To do this, a special fit is used as described below to create a surrogate for drag results. With this surrogate, we can take properties from arbitrary sections along the wing and use them to determine the overall drag due to compressibility effects during a wing analysis. Parasite drag effects are then added using low-fidelity methods for the full wing. We intend to expand the airfoil optimization to include parasite drag in the future with the inclusion of the Reynolds number.

The basic work flow up to surrogate creation is shown in Figure 1. This process would occur before a wing or aircraft optimization loop. The parameters shown apply to Euler flow, as explained in the following subsection.

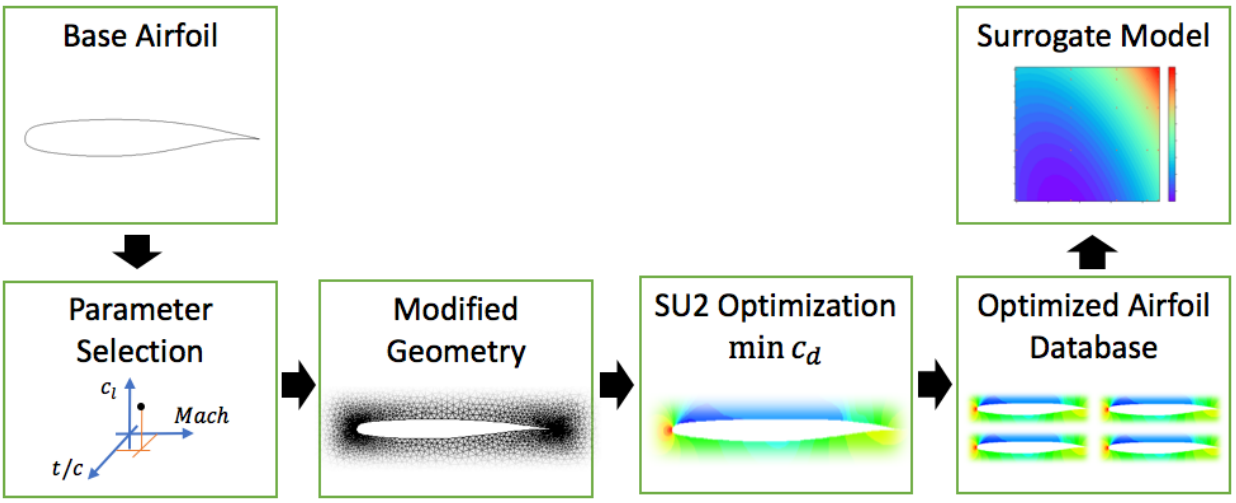

Figure 1: Surrogate Generation Flow

B. Airfoil Optimization

Airfoils are initially optimized in Euler flow with the relevant parameters of t/c, section c_l, and Mach. In order to build a surrogate that will provide accurate values when queried with any combination of these values, a substantial number of points needs to be available to fit. To accomplish this, points are drawn from half a distribution of cosine spaced values such that the spacing is tighter near the areas where we expect high amounts of variation. For this framework, that means spacing is tighter at high c_l, high t/c, and high Mach number, since we except compressibility drag to increase sharply at those extremes. This sampling procedure is described by equations 7-9, with n as the number of desired sampling points in a given dimension, y as the condition variable to be sampled, and i from $n-1$ to $N-1$.

$$N = 2n - 1 \tag{1}$$

$$y_{spacing}[i-(n-1)] = (1 - \cos(\pi i/(N-1))) - 1 \tag{2}$$

$$y_{sampling} = y_{spacing}(y_{max} - y_{min}) + y_{min} \tag{3}$$

Once the points to be fit are chosen, an optimization is run using SU2's Hicks-Henne bump procedure, with SNOPT[4] as the optimizer. This procedure works by deforming bumps on specified sections of the airfoil, which modify the surface of the airfoil. In this case, 19 bumps are specified along the top and bottom surfaces and are spaced evenly along the airfoil's unit length at intervals of 0.05.

There are four constraints used in the optimization besides the variables bounds (which exist primarily to prevent divergence and are not meant to be active). The first is the c_l constraint. This is handled differently than the other constraints in that it is enforced directly in the SU2 call. This is done by varying the angle of attack of the current airfoil iteration until the desired lift coefficient is achieved. The second constraint is the maximum thickness to chord, which is calculated after each SU2 run. The third is a moment constraint. This constraint is determined by running the base airfoil and determining the moment coefficient. This coefficient is then set as the maximum with the intention of producing an airfoil that will not create a moment with more pitch down than the initial airfoil. The final constraint is the requirement that the airfoil surfaces do not cross through the surfaces of a similar airfoil at reduced thickness. This effectively creates a skeleton of the initial airfoil and is used to ensure that the airfoil does not violate other implicit constraints that may be important in wing design (i.e. manufacturability). More details on the creation of this skeleton follow. The mathematical formulation of this optimization is given in equation 4.

$$
\begin{aligned}
\underset{\mathbf{x}}{\text{minimize}} \quad & c_d(\mathbf{x}) \\
\text{subject to} \quad & c_l(\mathbf{x}) = given\ c_l \\
& c_m(\mathbf{x}) \leq initial\ c_m \\
& t/c(\mathbf{x}) \leq t/c_{max} \\
& surface\ violation(\mathbf{x}) \leq 0 \\
& lb_i \leq x_i \leq ub_i,\ i \in \{1, ..., n\} \\
& \mathbf{x} \in \mathbb{R}^n
\end{aligned} \tag{4}
$$

To create the airfoil mesh and determine the surface bound curves, the surface of the initial airfoil is made by taking a parent airfoil and modifying the surfaces such that the maximum thickness is the same as the maximum thickness constraint. These surfaces are then fed to an automated Pointwise script which creates and exports the mesh to SU2 format. The inner bound is created based on the points in this mesh such that the bound surfaces are 10% closer to the camber line than the airfoil surfaces. This bound in relation to an initial airfoil is shown below in Figure 2.

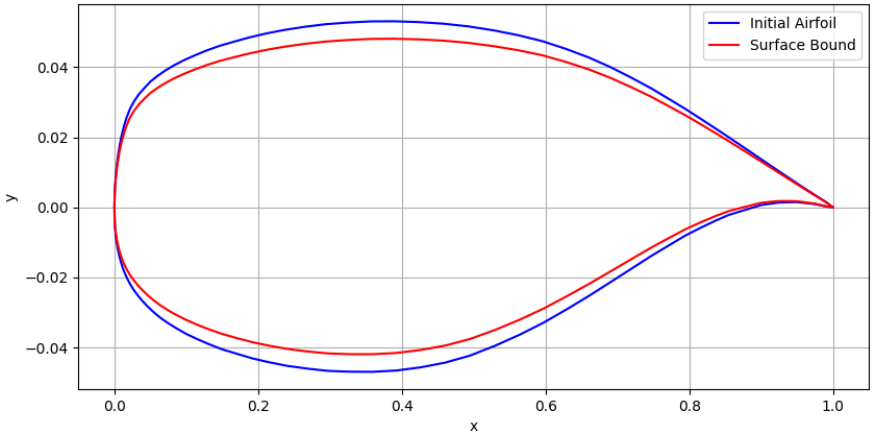

Figure 2: Example Initial Airfoil and Surface Bound

C. Surrogate Creation

In order to provide airfoil drag data at every flight condition, some form of surrogate must be made such that this information can be estimated at points that have not previously been sampled. In addition, there are occasional points in the optimization set that provide erroneous values due to various numerical issues, and numerical noise can contribute to optimization values that do not perfectly follow a simple curve.

The surrogate showing the most promise is constructed as polynomial fit of the data in the t/c and c_l dimension, followed by a power law fit in the Mach number. This was inspired by the 3D compressibility drag fit for modern subsonic wings used by SUAVE[2] under the assumption that the behavior of our own optimal airfoils in these dimensions would be somewhat similar. Equations 5 and 6 show how this is set up. Scipy's[5] curve fit function is used to find the optimal parameters for the fit after initial guesses are determined manually.

$$c_{d_{base}} = K_1 + K_2 c_l + K_3(t/c) + K_4(t/c)^2 + K_5(t/c)c_l + K_6 c_l^2 \tag{5}$$

$$c_{d_c} = c_{d_{base}}(Mach)^{K_7} \tag{6}$$

Once the initial surrogate is made, we seek to eliminate unreliable optimization results from the fit. We assume that these optimizations give the resulting c_d as much higher than other points nearby, so drag results are removed if they are higher than the surrogate drag by more than 50%. After these points are removed, the surrogate is refit using the remaining points and the final parameters are saved.

D. Aerodynamic Integration

Once a surrogate is created from the optimized airfoils, it is possible to use that data to construct a full wing. This is done by taking sections of the wing, extracting the t/c, c_l, and Mach number, then using the surrogate along with other methods to find the drag at various points along the wing. Airfoil compressibility drag from the surrogate is integrated along the wing, parasite drag is estimated using the standard parasite drag methods in SUAVE, and induced drag is determined based on given lift distribution. This lift distribution can be pre-specified or optimized. Procedures for this integration have been implemented for the case of a swept wing. The details for integration of each drag component are given below.

1. Compressibility

In the inviscid 2D case, the drag captured by the surrogate is entirely due to compressibility effects (and some small effects due to the numerical method used). As such, for every section of the wing, the t/c, c_l, and Mach number are found. The segment between two specified sections is then broken into a given number of smaller segments, and the t/c, c_l, and Mach number are found at new intermediate sections by interpolating the original sectional values. This is done with linear interpolation.

To convert these values to those for a swept wing, we use a set of simple transformations based on the sweep angle.[6] We expect that these will provide sufficient accuracy to test our model, but will be enhanced in the future to provide higher fidelity.

$$M_\perp = M \cos \Lambda \tag{7}$$

$$c_{l\perp} = c_l / \cos^2 \Lambda \tag{8}$$

$$(t/c)_\perp = (t/c) / \cos \Lambda \tag{9}$$

Once the sectional values for all the newly created sections are determined these are input into the surrogate to find each sectional drag coefficient. In some cases the surrogate may return a slightly negative value, which is instead then set to zero. These are then integrated along with the section chord lengths to find the total compressibility drag along the wing.

2. Parasite

Since this iteration of the process does not include viscous effects in the drag surrogate, parasite drag is drawn from a lower fidelity method. This method is drawn from the method in SUAVE and determines the skin friction on each segment based on Reynolds number of the segment's mean aerodynamic chord, and determines the total parasite drag based on that number. Details about the how these values are calculated can be found in the SUAVE capabilities paper.[2]

3. Induced

Induced drag is determined using a panel method with a specified c_l at each section, based on a Treffz-plane method.[7] Additional sections are also added between the main specified sections with the c_l linearly interpolated. This Treffz-plane method is used rather than lifting-line or other no-sweep methods because of the application to swept wings. The implementation was verified by ensuring that optimization of an arbitrary c_l distribution resulted in an elliptical lift distribution.

IV. Results

A. Airfoil Optimization Example

An example of the airfoil optimization procedure is shown below. The initial geometry is the NLR-7301 airfoil scaled down to match the required thickness to chord. This parent NLR-7301 is used in all following optimizations and was chosen since it was a readily available airfoil that was created for transonic flow. The optimization is set up using Mach 0.8, t/c of 0.1, and c_l of 0.6. The mesh for this airfoil is shown below in Figure 3. A relatively coarse mesh is used as this provides greater robustness in the optimization procedure.

The farfield is circular and 30 chord lengths from the origin. Figure 4 shows how the airfoil surface geometry has changed, and Figures 5 and 6 show how the pressure near the airfoil has changed due to these effects, removing the significant shock.

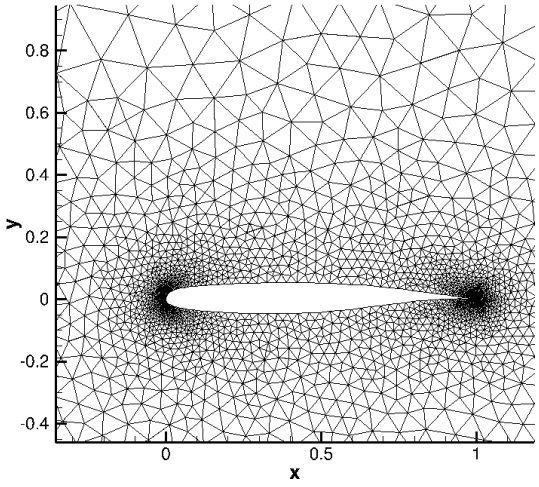

Figure 3: Base Airfoil Mesh

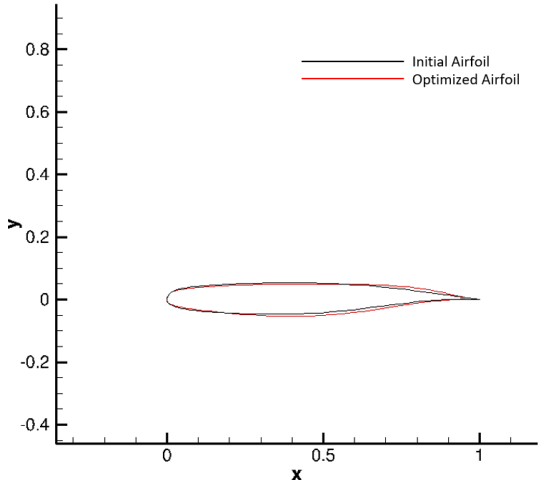

Figure 4: Airfoil Surface Difference

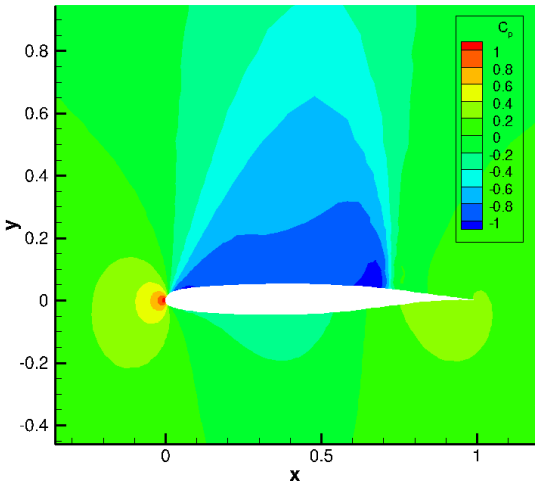

Figure 5: Base Airfoil, $c_d = 0.0128$

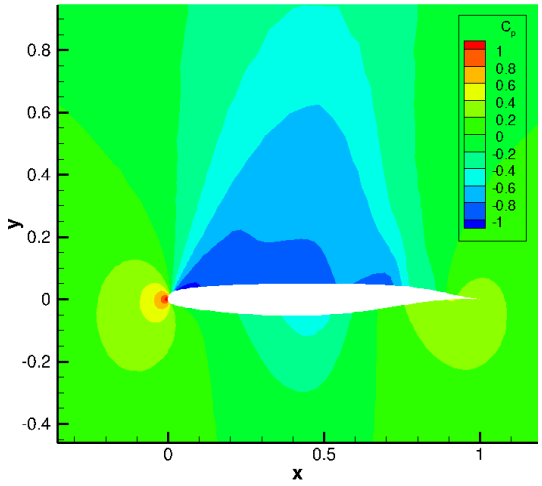

Figure 6: Optimized Airfoil, $c_d = 0.0041$

B. Optimization and Surrogate Creation

Points to be used in optimization are selected using cosine spacing as described in Section III. The condition bounds are chosen as in Table 1, resulting in a point distribution at each sampled Mach number as shown in Figures 7. This same spacing is applied in all three dimensions, creating a distribution with points bunched at high t/c, c_l, and Mach.

Table 1: Flight Condition Variable Bounds

Variable	Lower Bound	Upper Bound
Coefficient of Lift	0.00	0.90
Thickness to Chord	0.06	0.14
Mach Number	0.70	0.85

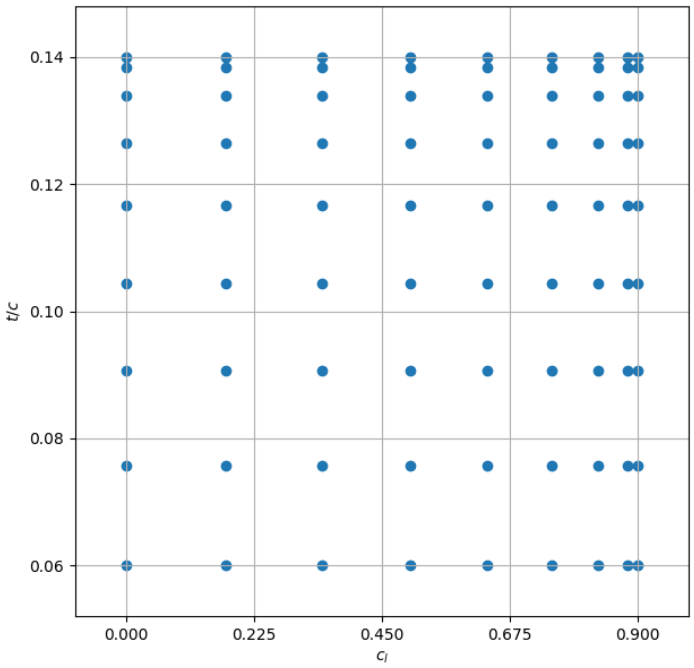

Figure 7: Parameter Spacing at Fixed Mach

Optimizing these points provides drag coefficient distributions that can be plotted as surfaces when one of the parameters is held fixed. Figures 8 and 9 give a general idea of the characteristics of the surfaces. As expected, the numbers tend to increase with increasing lift coefficients and thicknesses.

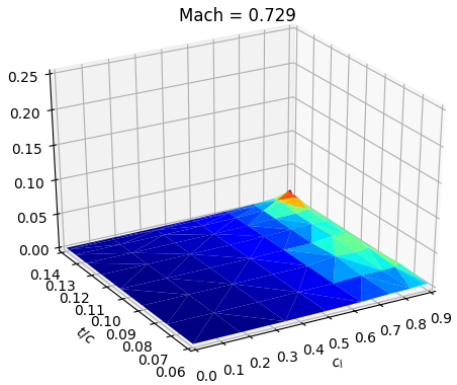

Figure 8: Results at Mach = 0.729

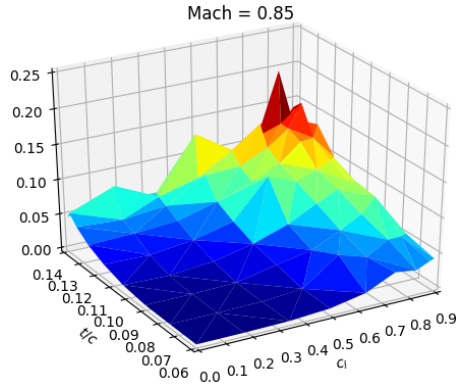

Figure 9: Results at Mach = 0.85

We then use the fitting algorithm described in Section III, which produces a surrogate with the following slices. The coefficients describing these are given in Table 2.

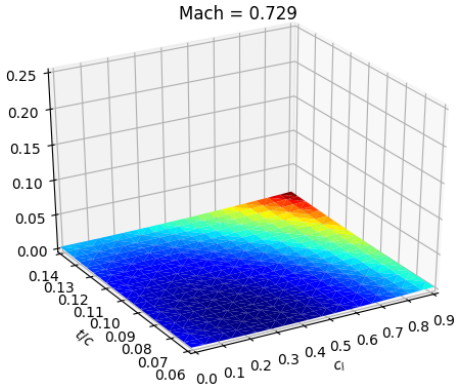

Figure 10: Surrogate at Mach = 0.729

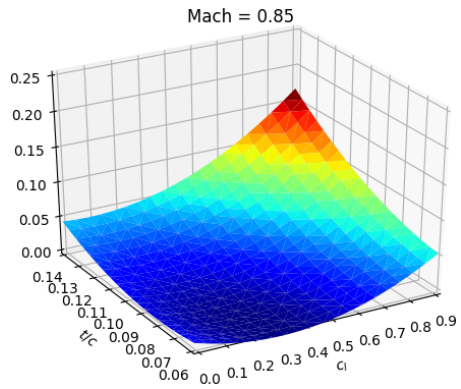

Figure 11: Surrogate at Mach = 0.85

Table 2: Coefficients for Surrogate

Coefficient	Value	Coefficient	Value	Coefficient	Value
K_1	1.76	K_4	22.9	K_7	19.0
K_2	-3.99	K_5	259		
K_3	-42.7	K_6	4.11		

C. Lift Distribution Optimization

With a completed surrogate model available, we can now add it to the wing analysis and optimize the lift distribution to minimize drag while including compressibility effects. Sections of the wing are chosen as control points for the lift distribution. The initial wing in this optimization is a simple rectangular wing with dimensions similar to that of a 737. The leading and trailing edges of each section are marked on the wing planform in Figure 12. The sections are more tightly spaced toward the wingtip in order to better capture the expected optimal lift distribution. Note that although only half the wing is shown, the full wing is used in the calculations.

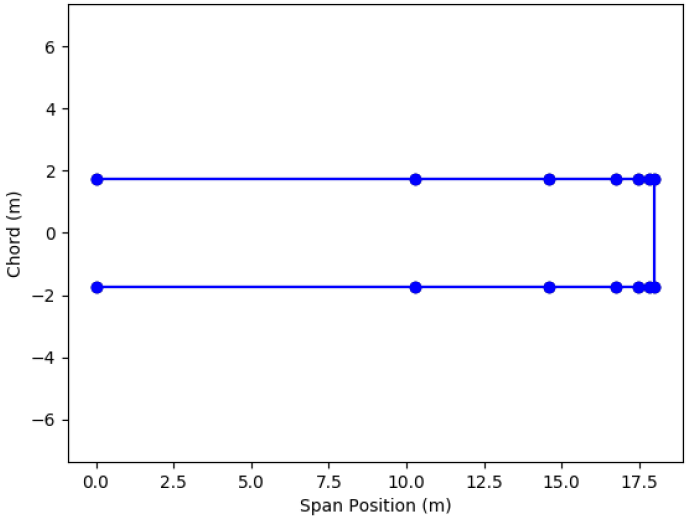

Figure 12: Wing Planform with Section Markers

To perform the optimization, a given lift is prescribed (chosen to be similar to the lift necessary for a

737-sized aircraft) and total drag is minimized. The optimization setup is shown in equation 10 with $\mathbf{x}$ as the distribution of c_l.

$$\begin{aligned} \underset{\mathbf{x}}{\text{minimize}} \quad & c_d(\mathbf{x}) \\ \text{subject to} \quad & L(\mathbf{x}) = 800,000N \\ & lb_i \leq x_i \leq ub_i, \ i \in \{1, ..., n\} \\ & \mathbf{x} \in \mathbb{R}^n \end{aligned} \tag{10}$$

This optimization is performed at Mach 0.75 once ignoring compressibility drag and once with compressibility drag. The resulting distributions are shown in Figure 13 This shows that the c_l distribution shifts outward with compressibility effects, which we can expect due to higher drag at higher lift coefficients pushing those lift coefficients to lower values. The design variable bounds are not active. Note that the somewhat irregular shape of the induced drag distribution is caused by linear interpolating of the lift between specified sections, but does not have a significant impact on the total induced drag number. The b used in computing span position is half the total span.

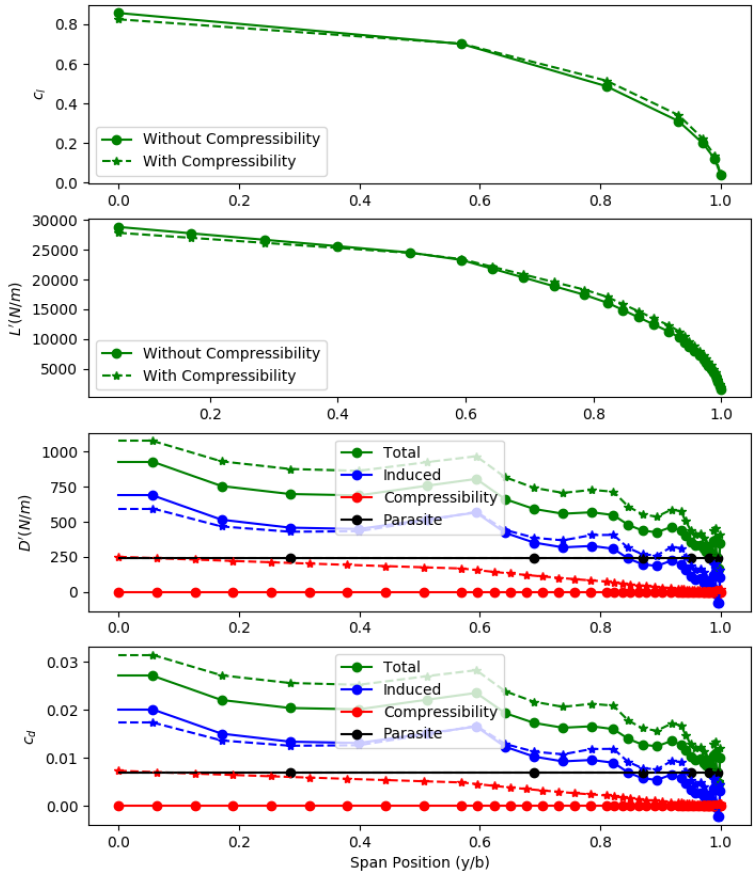

Figure 13: Force Distribution with and without Compressibility Drag

D. Optimization Including Planform Changes

Next the optimization is performed again taking planform changes into consideration. To do this, the taper ratio, root chord length, and sweep are allowed to vary. Additionally the wing is not allowed to become heavier than the base wing would be at 30 degrees of sweep, as calculated by the wing weight correlation used in SUAVE.[2] These parameters were chosen to demonstrate the ability to vary the planform within a range where weight estimation would still be useful. The modified optimization is given in Equation 11, with x now including the taper ratio, root chord length, and sweep. The resulting distributions and planform are

shown in Figures 14 and 15. This shows a lift distribution that remaining largely elliptical, but a change in c_l distribution such that lower values are seen in segments with greater areas. The final taper ratio, root chord length, and sweep are 0.13, 9.9 m, and 28 degrees respectively. We note that the planform would not change from the base zero sweep without including compressibility effects. The design variable bounds are not active.

$$\begin{aligned} \underset{\mathbf{x}}{\text{minimize}} \quad & c_d(\mathbf{x}) \\ \text{subject to} \quad & L(\mathbf{x}) = 800,000N \\ & W(\mathbf{x}) \leq W_{initial}(\mathbf{x}) \\ & lb_i \leq x_i \leq ub_i, \ i \in \{1, ..., n\} \\ & \mathbf{x} \in \mathbb{R}^n \end{aligned} \tag{11}$$

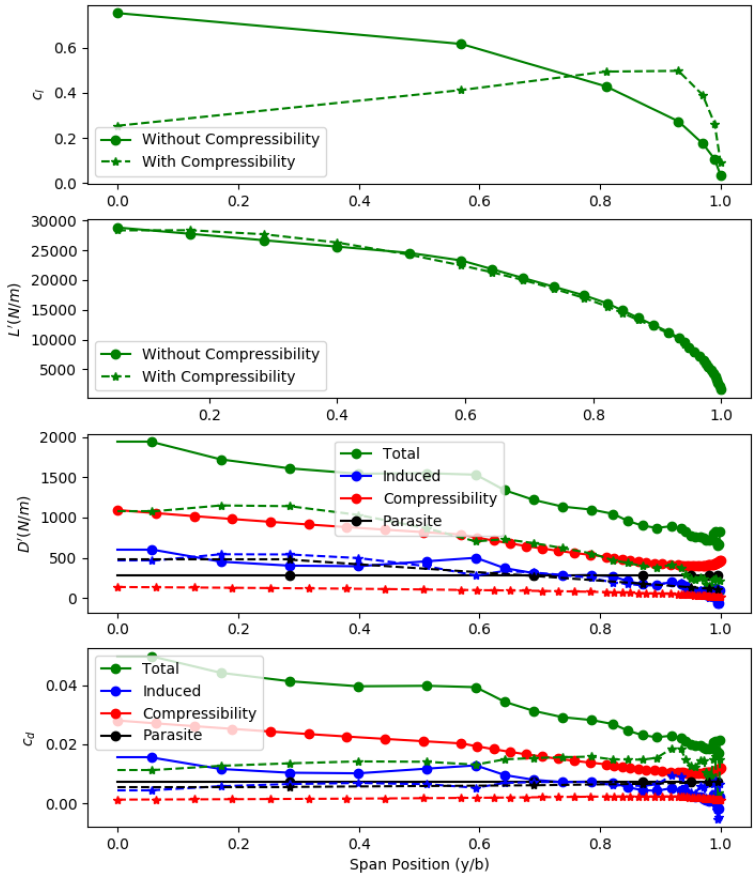

Figure 14: Force Distribution with and without Sweep

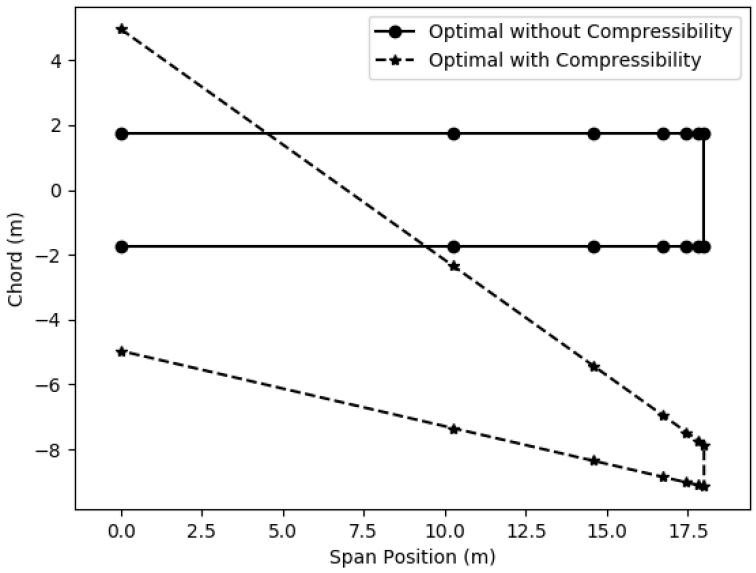

Figure 15: Wing Planform with with and without Sweep

V. Summary

A method to compute 3D wing aerodynamic properties using optimized 2D airfoils is being developed for use in the conceptual design process. Here we explain the capabilities we have used, the methods developed thus far, and show results of optimizations with these methods. We have started with Euler optimizations and a basic swept wing to test the framework. This shows that the methods are capable of producing the expected results. We will continue to develop the methods for swept wings and incorporate viscous effects. We expect that this will give results similar to an optimized 3D wing, and will test against that case to verify.

Acknowledgments

Timothy MacDonald would like to acknowledge the support of the Department of Defense (DoD) through the National Defense Science & Engineering Graduate Fellowship (NDSEG) Program.

References

[1]Palacios, F., Colonno, M. R., Aranake, A. C., Campos, A., Copeland, S. R., Economon, T. D., Lonka, A. K., Lukaczyk, T. W., Taylor, T. W. R., and Alonso, J. J., "Stanford University Unstructured (SU2): An open-source integrated computational environment for multi-physics simulation and design," *51st AIAA Aerospace Sciences Meeting and Exhibit*, Grapevine, TX, January 2013.

[2]Lukaczyk, T., Wendorff, A. D., Botero, E., MacDonald, T., Momose, T., Variyar, A., Vegh, J. M., Colonno, M., Economon, T. D., Alonso, J. J., Orra, T. H., and Ilario da Silva, C., "SUAVE: An Open-Source Environment for Multi-Fidelity Conceptual Vehicle Design," *16th AIAA/ISSMO Multidisciplinary Analysis and Optimization Conference*, Dallas, TX, June 2015.

[3]Van der Velden, A., Kelm, R., Kohan, D., and Mertens, J., "Application of MDO to Large Subsonic Transport Aircraft," *38th AIAA Aerospace Sciences Meeting and Exhibit*, Reno, NV, January 2000.

[4]Gill, P., Murray, W., and Saunders, M., "SNOPT: An SQP Algorithm for Large-Scale Constrainted Optimization," *Society for Industrial and Applied Mathematics*, Vol. 47, No. 1, February 2005, pp. 99 – 131.

[5]Jones, E., Oliphant, T., Peterson, P., et al., "SciPy: Open source scientific tools for Python," 2001–.

[6]Mariens, J., Elham, A., and van Tooren, M. J. L., "Quasi-Three-Dimensional Aerodynamic Solver for Multidisciplinary Design Optimization of Lifting Surfaces," *Journal of Aircraft*, Vol. 51, No. 2, March-April 2014.

[7]Smith, S., "Treffz-Plane Drag Minimization at Transonic Speeds," *SAE Technical Paper Series*, , No. 971478, April 1997.